Overview and Interpretation of L-H Threshold Experiments on JET with the ITER-like Wall

E Delabie[1], C F Maggi[2], H Meyer[3], T M Biewer[4], C Bourdelle[5], M Brix[3], I Carvalho[6], P Drewelow[7], N C Hawkes[3], J Hillesheim[3], A G Meigs[3], L Meneses[6], F Rimini[3], P Siren[8], E Solano[9], M Stamp[3] and JET contributors*

JET-EFDA, Culham Science Centre, Abingdon, OX14 3DB, UK
[1]FOM-DIFFER, Nieuwegein, The Netherlands
[2]MPI für Plasmaphysik, Garching, Germany
[3]CCFE, Culham Science Centre, Abingdon, UK
[4]Oak Ridge National Laboratory, Oak Ridge, Tennessee, USA
[5]CEA, IRFM, F-13108 Saint-Paul-lez-Durance, France
[6]Associacao EURATOM-IST, Lisboa, Portugal
[7]MPI für Plasmaphysik, Greifswald, Germany
[8]Association EURATOM-Tekes, FIN-02044 VTT, Finland
[9]Asociación EURATOM/CIEMAT, Madrid, Spain
Corresponding Author: ephrem.delabie@jet.efda.org

Abstract:
The expected threshold power (P_{L-H}) required to access H-mode operation on ITER is extrapolated from a multi-machine scaling that is strongly weighted to a dataset of JET carbon wall discharges [1]. Experiments on JET with the Be/W wall show a minimum in P_{L-H} as function of density and a favorable reduction in the threshold power of 30% at medium to high densities [2]. The carbon wall threshold can be recovered with nitrogen injection. An increase in the threshold power by up to a factor 2 and a reduction of the density at which the minimum occurs was found when the outer strike point position was moved from the horizontal to the vertical target. The existence of a critical $\min(E_{r,dia})$ is consistent with the threshold data from each of the divertor configurations but does not explain the differences between them. The observation of a strong asymmetry between the inner and outer divertor that develops during a power ramp is correlated with the L-H threshold in the high density branch and indicates a direct effect of the scrape off layer or divertor conditions on the threshold. This mechanism also provides a qualitative explanation for dithering L-H transitions.

1 Introduction

H-mode operation is foreseen as the baseline scenario for high performance discharges on ITER and it is important that this scenario can be accessed relying on external heating in the early phases of ITER operation. The expected power that is required to reach H-mode is extrapolated from a multi-machine database [1] and for sufficient high density this scaling is an increasing function of line averaged density ($\propto \langle n_e \rangle^{0.717}$). At full field (5.4T) and in deuterium, a threshold power of ≈52MW is expected at a density of 0.5 10^{20} m^{-3} [1] for an available heating power of 73MW, but with large uncertainties in the extrapolation. Because of this density scaling the ITER scenario foresees to enter H-mode at low density and then relies on alpha heating to keep the plasma in H-mode as the density is increased to 1.0 10^{20} m^{-3} for which the expected threshold power reaches ≈86MW.

The scaling law, which is used as a guidance for development of ITER plasma scenarios, is strongly biased by a large contribution of carbon wall JET (JET-C) pulses to the threshold

*See the Appendix of F. Romanelli et al., Proc. 25th IAEA Fusion Energy Conference 2014, Saint Petersburg, Russia

database as being the nearest device for extrapolation to ITER. This has motivated comparison discharges between JET-C and JET with the beryllium/tungsten wall (JET-ILW) [2]. A general description of the experiments in this paper and the results of the JET-C to JET-ILW comparison are summarized in section 2.

In past JET-C experiments, a strong effect of divertor configuration on the threshold has been observed and is investigated in more detail in JET-ILW in section 3. Section 4.1 shows a correlation between the high density branch of the L-H threshold and changes in divertor plasma conditions that could provide a qualitative explanation for the effect of the divertor configuration. This also provides a possible explanation for dithering L-H transitions as reported in section 4.2. Section 5 shows the effect of nitrogen injection, which has been used to investigate the effect of low Z impurities as indicated by the difference between the JET-C and JET-ILW datasets.

2 Comparison between JET-C and JET-ILW

All data shown in this paper come from discharges in which the input power has been linearly increased at a rate of 1MW/s with feedback control on the density to achieve a constant density in the L-mode phase. All discharges are single null with $B \times \nabla B$ towards the divertor. The threshold power, $P_{L-H} = P_{\Omega} + P_{ICRH} + P_{NBI} - dW_{dia}/dt$, has been taken in the L-mode phase during the last 70ms before the transition. The discharges at 3T are performed with NBI heating, while the 2.4T pulses are mainly heated with ICRH, except for those on vertical target configuration. The dataset at 1.8T is mixed between NBI only or ICRH only. Apart from an additional increase in core radiation with ICRH at low density, the heating method has no effect on the threshold and data from mixed heating schemes are shown without distinction [2].

The threshold power P_{L-H} is not corrected for the bulk radiation for easy comparison with the ITPA scaling law. This does not qualitatively change any of the observations reported here. The main effect of using $P_{sep} = P_{L-H} - P_{rad,bulk}$ instead of P_{L-H} is a reduction in steepness of the increase in threshold power at low density (see [2]).

In order to evaluate the change in L-H threshold due to the changeover from the carbon to the beryllium/tungsten ITER-like wall, discharges have been carried out with identical plasma shape, B_t and I_p [2]. Figure 1(a) shows the measured threshold power against line averaged density for JET-C and JET-ILW discharges at 1.8T/1.7MA. The JET-ILW experiments show a minimum in the threshold power as function of density. This was not observed with the current MkII-HD divertor in JET-C, but this minimum was seen before on the carbon wall JET with the MkII-GB divertor (divertor with septum) [3]. The JET-C data follow the ITPA scaling whereas the JET-ILW pulses show a favorable reduction of 30% in the high density branch. Combining these datasets with a scan in the same configuration at 2.4T/2MA (shown in fig. 2(a)) and at 3T/2.75MA, shows that the $B_t^{0.803}$ scaling from the ITPA scaling law still fits very well in the high density branch. The density dependence is not matched well by reducing the pre-factor to the scaling law or exponent. Shifting the entire scaling law by adding an offset to the density scaling, but keeping the $\langle n_e \rangle^{0.717}$ dependence, gives a better fit.

The existence of a density at which P_{L-H} has a minimum has been observed on many machines. H-mode access through the minimum could be a viable scenario for ITER, if the density at the minimum is accessible. In [2], a $B_t^{4/5}$-scaling based on the JET data (at q_{95}=3.3-3.7) was found. The physical mechanism separating the low and high density branches is an important open question. In [4] electron-ion decoupling is proposed as a mechanism, and a scaling proportional to $B_t^{0.62} I_p^{0.34}$ is derived. The decrease in the minimum density by lowering

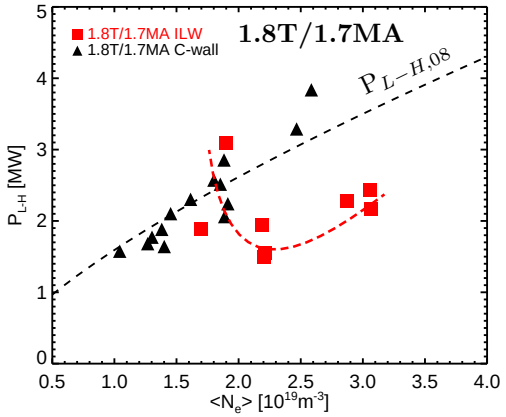

(a) L-H threshold power from comparison discharges between JET-C and JET-ILW. The black dashed line corresponds to the ITPA scaling law [1]

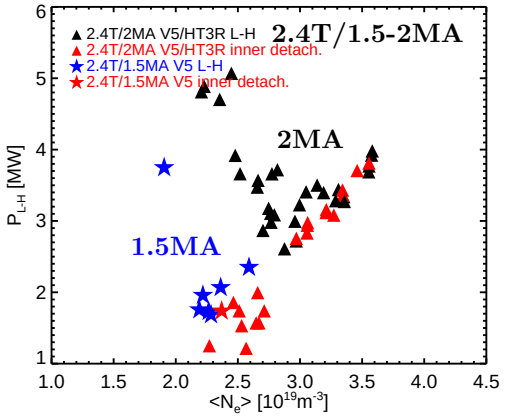

(b) L-H threshold at 2MA and 1.5MA (2.4T).The lowest density point at 1.5MA remained in L-mode. The red symbols indicate the power at which the inner divertor leg detaches (see sect.4.1).

FIG. 1: P_{L-H} as function of line averaged density. The inner strike point is on the vertical target and the outer on the horizontal target. The estimated error on P_{L-H} is mainly systematic (≈15%).

the plasma current is also observed on JET, as shown in fig. 1(b). The effect of the current is only visible in the low density branch and the scaling from [4] is in reasonable agreement with the JET data. No clear sign of decoupling between electrons and ions is observed however as $T_e \approx T_i$ in the pedestal even at lowest density. The pulses with NBI used rather modest beam voltages (70-100keV with 50% of the power in the E/2 and E/3 fractions) which results in 40-70% ion heating. Therefore, under these circumstances, decoupling between electrons and ions would not be expected to increase the threshold at low density, but this still needs to be confirmed by heat flux analysis. As yet, the physical mechanism for the existence of a low and high density branch has not been unambiguously established.

3 Effect of divertor configuration on the L-H threshold

The magnetic configuration in the divertor is known to affect the L-H threshold on JET as shown by comparison between different divertors (Mk0 to MkII) and by changing the strike point and X-point positions [5, 6, 3]. On JET-C P_{L-H} was found to increase with X-point height and decrease with divertor closure, which could be interpreted as an effect associated with changes in the recycling pattern. Given the different recycling properties of tungsten and graphite, experiments were conducted to investigate the effect of divertor configuration in the ILW environment. Fig. 2(a) shows P_{L-H} for 3 density scans at 2.4T/2MA using the divertor configurations shown in fig. 2(b). The main plasma shape has been kept as similar as possible. The configurations labelled V5 and V5L have one strike point on the horizontal target and one on the vertical target. The V5L configuration has a lower threshold than the V5 configuration and mainly differs in having the inner strike point higher up onto the inner divertor target creating a higher lower triangularity. The vertical target configuration (labelled VT in fig. 2) has a threshold almost twice as high as the V5 configuration [7], bringing it close to the ITPA scaling. No minimum in P_{L-H} was found within the experimentally accessible density range at 2.4T. At 3T the minimum was recovered at lower density than in the semi-horizontal configuration, confirming that empirically the P_{L-H} curve is shifted as function of density.

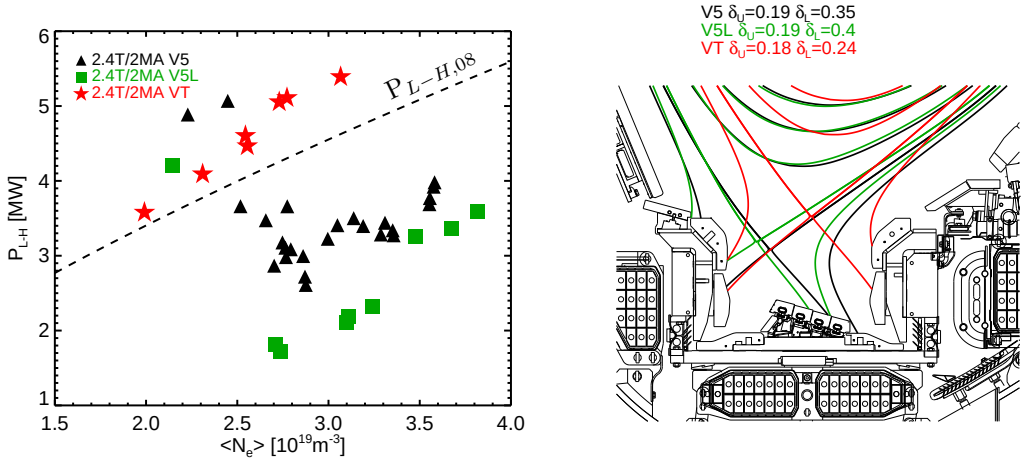

(a) L-H threshold at 2.4T/2MA for the three divertor configurations shown in fig. 2(b). The black dashed line corresponds to the ITPA scaling law [1].

(b) Equilibria showing the strike point and X-point positions for three different divertor configurations.

FIG. 2: Effect of the divertor configuration on the L-H threshold.

Differences in bulk radiative power losses are not enough to account for the large differences between the threshold in the different divertor configurations. The accepted view on the L-H transition is that a sustained transition is triggered by the $E_r \times B$ velocity shear. There is an increasing amount of evidence, mainly from AUG [8, 4], that the radial electric field in the L-mode edge is driven by the density and temperature gradients of the main ion species. This means that for main ions the first term in the force balance equation ($E_r = 1/Zq_i \, \nabla p_i/n_i - v_i \times B$) is dominant. On JET, the measured toroidal rotation at the position of the pressure gradient is indeed low or only has a small gradient and the modelled main ion poloidal rotation (from NCLASS [9]) is negligible. Therefore, we have tested if the observed differences in threshold could be explained by differences in the edge temperature or density profiles caused by e.g. changes in the fuelling profiles or edge radiation. According to this hypothesis, more power would be required to reach the same radial electric field shear. In order to obtain the main ion diamagnetic term to test this assumption, we have fitted the edge electron density profiles (assuming $n_i \approx n_e$) and the edge electron temperature profiles (all studied discharges which have edge CXRS measurements show $T_i = T_e$ in the pedestal). Thomson scattering data was used for the relative alignment of the temperature and density profiles. The profiles have been fitted using modified tanh functions [10] extended with splines. Fig. 3(a) shows the edge electron and ion temperatures and fig. 3(b) show the corresponding minima in $E_{r,dia}$ (as a proxy for the shearing rate). The density profiles are similar between the divertor configurations, but the temperature at the transition is significantly higher in the vertical target configuration. The higher temperatures translate to a deeper E_r well. The same conclusions hold for the dataset at 3T for which T_i is available in both configurations.

For each of the divertor configurations, $\min(E_{r,dia})$ is similar over the density range, consistent with the assumption of a critical E_r driven by the ion channel [4]. The difference between the divertor configurations however cannot be explained by changes in the profiles. A possible explanation is that the boundary condition for E_r in the scrape off layer is altered between the different divertor configurations. This would change the shear in the outer part of the E_r well.

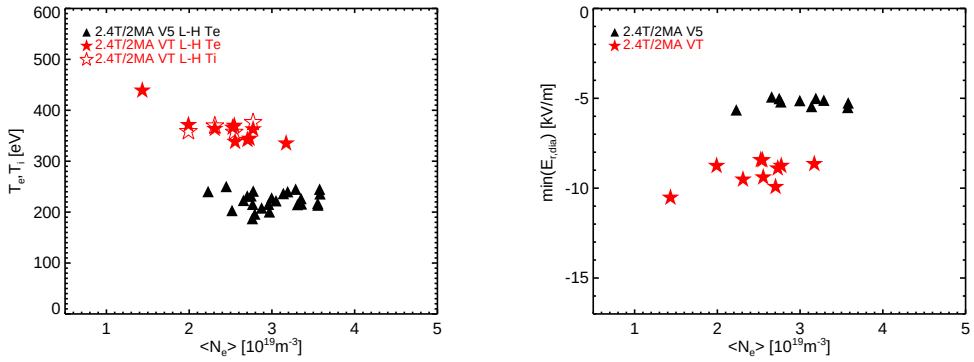

(a) T_e from ECE and T_i from CXRS (for beam heated pulses) before the transition at the location where the pedestal top forms.

(b) Minimum in the diamagnetic contribution to the radial electric field based on the electron kinetic profiles (T_e=T_i).

FIG. 3: Edge temperarture and minimum in the diamagnetic contribution to E_r for horizontal (black) and vertical (red) target configurations.

4 Dynamics of L-H transitions

4.1 Correlation between divertor plasma conditions and the L-H threshold

The slow power ramps used in L-H experiments show gradual and sudden changes in divertor conditions during the L-mode phase. At medium to high density, the D_α emission from the inner divertor is initially similar to the emission from the outer divertor, but as the inner emission gradually increases, the outer D_α emission decreases during the power ramp. This is consistent with Langmuir probe data that show a decrease in density at the outer divertor and a gradually increasing density at the inner divertor. This developing asymmetry in the divertor could be the effect of drifts in either the divertor or scrape off layer [11]. At a critical input power (at around 14.18s in fig. 4(a)) the asymmetry reaches a point at which the inner divertor partially detaches, which is most clearly observed by the strong increase in deuterium radiation and drop in saturation current on the Langmuir probes. The temperature at the inner strike point drops below a level at which it can still be measured reliably while at the outer strike point the temperature increases to about 25eV. The ratio D_δ/D_α in the inner divertor increases by a factor 2. This transition is often oscillatory, triggered by the heat flux from sawtooth crashes, and is likely the same phenomenon as described in [12], called 'divertor oscillations'. The only difference between the observation described in [12] and those reported here is that we observe no change in the upstream profiles during these oscillations. These oscillations are commonly observed before the L-H transition in the high density branch, but less common in the vertical target configuration. Fig. 1(b) shows the power at the onset of the transition to the higher inner divertor recycling state. There is a clear correlation between the high density branch of the L-H transition and the onset of the divertor oscillations. For pulses around the minimum in P_{L-H}, the transition to the partially detached state takes place very early in the power ramp, just above the ohmic power level. At the highest density in the scan, the detachment of the inner strike point immediately triggers an L-H transition. There is also an indication that the reverse process, i.e. re-attachment of the inner divertor, can cause a back transition (see the dithering L-H transitions in sect. 4.2).

Fig. 5 shows the thresholds for the V5 and V5L configurations. In the V5L configuration, the oscillations were only clearly observed for two pulses as sometimes they are obscured by an initial power step preceeding the ramp. The high density branch of P_{L-H} shifts together

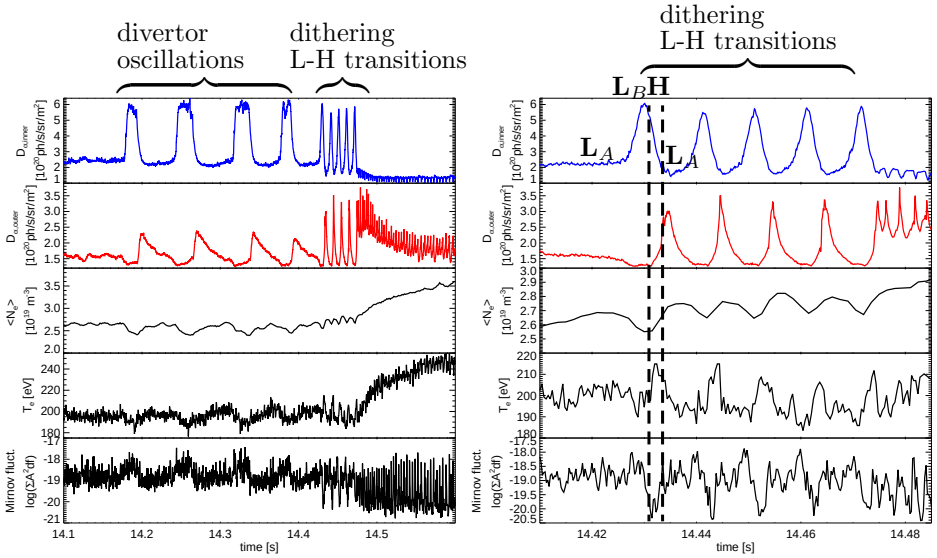

(a) Overview. (b) Zoom in on dithering L-H transitions.

FIG. 4: Timetraces of D_α, edge density, electron temperature and fluctuations on the inner mirnov coils during the divertor oscillation phase and dithering L-H transitions. The divertor oscillations are oscillations between states of lower and higher inner divertor recycling labelled L_A and L_B. The dithering L-H transitions start from the state L_B. After the short H-mode phase the plasma is back to state L_A.

with the divertor oscillations when comparing V5 and V5L. This indicates at least a corrrelation between both phenomena. In vertical target configuration the oscillations or inner detachment were not clearly observed at 2.4T before the L-H transition. If the inner detachment during the power ramp is caused by increasing drifts in the SOL/divertor, this could be an indication that these are much smaller in the vertical target configuration.

4.2 Dithering L-H transitions

L-H transitions in the high density branch are qualitatively different from low density transitions. At low density, the transition only causes a modest increase in confinement with the formation of a small temperature pedestal and high frequent (1-3kHz) M-mode oscillations [13]. At high density, the transition causes a direct and clear increase in both temperature and density gradients, but always goes through a dithering phase (110-140Hz) during which short H-mode phases are interleaved with longer L-mode phases. The dithering transitions are only found around the minimum in P_{L-H} and in the high density branch. Fig. 4(a) shows the evolution of such a transition. The plasma first goes through the divertor oscillations described in section 4.1, followed by a short dithering phase before entering a sustained H-mode regime. Fig. 4(b) shows the dithering phase in more detail. The H-mode phase is characterized by a fast increase in the temperature, an increase in pedestal density and a drop in magnetic fluctuations from an inner Mirnov coil integrated between 17 and 100kHz. The latter has proven to be a good indication of the L-H transition (this is also seen on DIII-D [14]). The reflectometer records a clear increase in density gradient during the H-mode phase [15]. All signals behave similar as the first few milliseconds of a sustained L-H transition. The dithering phase can be stable for seconds if the power is not increased.

The observation that the dithering only occurs in the high density branch and the ressemblance between the divertor oscillations and the dithering oscillations (fig. 4(a)), apart from

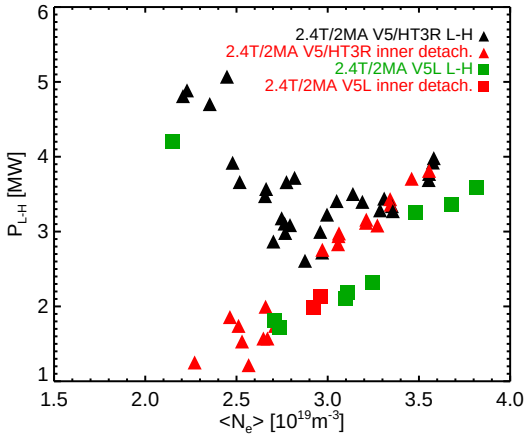

FIG. 5: L-H threshold (black/green) and threshold power (red) at which the inner divertor enters a high recycling regime for the V5 and V5L configurations (see fig.2(b)) at 2.4T/2MA.

the short H-mode phase, suggests that both phenomena could be related and this may help to understand the role of the divertor or SOL conditions. During the dithering phase, the transition to H-mode always starts from the phase with the increased inner divertor recycling and is labelled L_B in fig. 4(b). The inner D_α emission drops very soon after the transition into H-mode and reaches a level equal to the state with lower inner divertor emission which is labelled L_A in fig. 4(b) by the end of the H-mode phase. The outer D_α emission drops during the beginning of the H-mode phase and show a peak after the back transition. The next H-mode transition starts after the divertor plasma has gone back to state L_B. In view of the interpretation as divertor oscillations being a transition caused by drifts in the divertor or SOL that are driven by the heat flux entering the SOL, the short interruption of the heat flux as the pedestal starts forming could be the cause of the back transition to the divertor state L_A which appears less beneficial for H-mode access.

5 Effect of nitrogen injection on the L-H transition

To investigate the decrease in P_{L-H} from JET-C to JET-ILW, nitrogen has been injected in JET-ILW in the L-mode phase prior to the transition as it has similar radiative properties as carbon and increases Z_{eff} from the low ($\approx$1) values measured in JET-ILW to those typical of JET-C. The effect on the threshold power was first observed at 1.8T [16] and subsequently repeated at 3T for better diagnostic coverage. Fig. 6 show the measured threshold at 3T. The filled black stars show JET-ILW data at 2.75MA without nitrogen injection. The discharges with nitrogen injection were conducted at 2.5MA and are colored according to $\Delta \langle Z_{eff} \rangle$ which is dominated by the injected nitrogen. Because of the lower I_p, the low density branch is shifted to lower density. The plasma response to the injected nitrogen was slow and sometimes caused the plasma to fall back to L-mode multiple time as $\langle Z_{eff} \rangle$ increased during the power ramp. All observed transitions are plotted in fig. 6. The open symbols represent JET-C discharges. The JET-ILW datapoints with nitrogen injection at $\Delta \langle Z_{eff} \rangle$ >0.7 are close to the JET-C threshold, which implies that it is the change in impurity composition that is responsible for the reduction in P_{L-H}.

The change in threshold cannot be attributed to increased core radiation losses. The edge temperature is higher in the pulses with nitrogen injection, and consequently $\min(E_{r,dia})$ is deeper [16]. One possible explanation is a direct influence of Z_{eff} on the plasma turbulent properties in the pedestal [17]. A second possible explanation is a mechanism similar to the effect of the divertor configuration, where changes in the SOL/divertor alter the threshold directly.

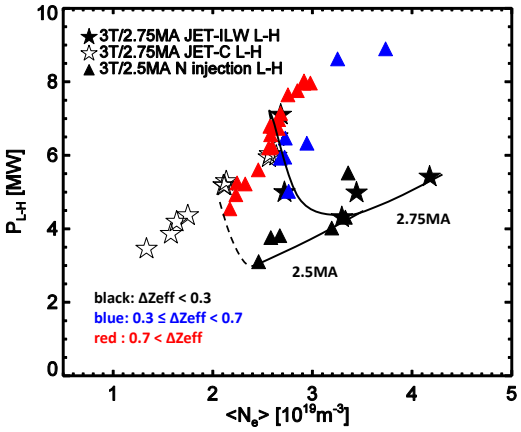

FIG. 6: L-H threshold power at 3T in semi-vertical divertor configuration for JET-C (open symbols) and JET-ILW discharges (solid symbols). The JET-ILW dataset at 2.75MA is without nitrogen injection, the data at 2.5MA is with nitrogen injection and is labelled according to ΔZ_{eff}. For some discharges, multiple transitions at increasing Z_{eff} were observed.

6 Conclusions

JET-ILW experiments show a minimum in the L-H threshold power as function of density, as seen on other machines and on JET-C with the MkII-GB divertor, and a reduction of the threshold by 30% in the high density branch. Both observations are potentially favorable for H-mode access on ITER. Nitrogen injection increases the threshold to JET-C values, demonstrating that the difference between JET-C and JET-ILW can be accounted for by the impurity composition. Experiments indicate that the density at which the minimum occurs depends on both impurity content and divertor configuration and was not accessible on JET-C with the current MkII-HD divertor geometry. Changes to the magnetic configuration in the divertor lead to changes in P_{L-H} up to a factor 2. Fits of the edge density and temperature profiles show agreement with the assumption of a critical, diamagnetic driven, E_r well (as proxy for the shearing rate) for each of the divertor configurations, but cannot explain the difference in P_{L-H} between them. A transition that creates a strong inner-outer asymmetry in the divertor plasma conditions is observed with the same power scaling as the high density branch of the L-H threshold and precedes the L-H transition at high density. This transition depends on the divertor configuration and hints to changes in the scrape off layer directly affecting the transition. A possibility is that SOL or divertor flows, that are thought to be responsible for the inner-outer divertor asymmetry, alter the boundary conditions for E_r in the scrape off layer and therefore the $E_r \times B$ shear.

Acknowledgement

This work was supported by EURATOM and carried out within the framework of the European Fusion Development Agreement. The views and opinions expressed herein do not necessarily reflect those of the European Commission.

[1] Y.R. Martin et al., *J. Phys.: Conf. Ser.* 123 (2008) 012033.
[2] C.F. Maggi et al., *Nucl. Fusion* 54 (2014) 023007.
[3] Y. Andrew et al., *Plasma Phys. Control. Fusion* 48 (2006) 479488.
[4] F. Ryter et al., *Nucl. Fusion* 54(8) (2014) 083003.
[5] L.D. Horton, *Plasma Phys. Control. Fusion* 42(5A) (2000) A37.
[6] Y. Andrew et al., *Plasma Phys. Control. Fusion* 46(5A) (2004) A87.
[7] H. Meyer et al., *Proceedings of the 41st EPS conference*, Berlin (2014).
[8] P. Sauter et al., *Nucl. Fusion* 52(1) (2012) 012001.
[9] W.A. Houlberg et al., *Phys. Plasmas* 4 (1997) 3230.
[10] R.J. Groebner et al., *Nucl. Fusion* 41(12) (2001) 1789.
[11] A.V. Chankin et al., *Journal of Nucl. Materials* 438 (2013) S463 - S466.
[12] A. Loarte et al., *Phys. Rev. Letters* 83 (18) (1999) 3657.
[13] E.R. Solano et al., *Proceedings of the 40th EPS conference*, Espoo (2013).
[14] K.H. Burrell et al., *Plasma Phys. Control Fusion* 31(10) (1989) 1649-1664.
[15] R. Sabot et al., *Proceedings of the 40th EPS conference*, Espoo (2013).
[16] C.F. Maggi et al., *Proceedings of the 41st EPS conference*, Berlin (2014).
[17] C. Bourdelle et al., *Nucl. Fusion Lett.* 54 (2014) 022001.